Impact of Al addition on the formation of Ni germanosilicide layers under different temperature annealing*

Xiao-Ran Meng(孟骁然)[1,2], Yun-Xia Ping(平云霞)[1,†], Wen-Jie Yu(俞文杰)[2], Zhong-Ying Xue(薛忠营)[2], Xing Wei(魏星)[2], Miao Zhang(张苗)[2], Zeng-Feng Di(狄增峰)[2], Bo Zhang(张波)[2,‡], and Qing-Tai Zhao(赵清太)[3]

[1] *Shanghai University of Engineering Science, Shanghai* 201600, *China*

[2] *State Key Laboratory of Functional Material for Informatics, Shanghai Institute of Microsystem and Information Technology, Chinese Academy of Sciences, Shanghai* 200050, *China*

[3] *Peter Grünberg Institute* 9 *(PGI* 9*-IT), and JARA-Fundamentals of Future Information Technology, Forschungszentrum Juelich, Juelich* 52425, *Germany*

(Received 17 March 2017; revised manuscript received 21 May 2017; published online 18 July 2017)

Solid reactions between Ni and relaxed $Si_{0.7}Ge_{0.3}$ substrate were systematically investigated with different Al interlayer thicknesses. The morphology, composition, and micro-structure of the Ni germanosilicide layers were analyzed with different annealing temperatures in the appearance of Al. The germanosilicide layers were characterized by Rutherford backscattering spectrometry, cross-section transmission electron microscopy, scan transmission electron microscopy, and secondary ion mass spectroscopy. It was shown that the incorporation of Al improved the surface and interface morphology of the germanosilicide layers, enhanced the thermal stabilities, and retarded the Ni-rich germanosilicide phase to mono germanosilicide phase. With increasing annealing temperature, Al atoms distributed from the $Ni/Si_{0.7}Ge_{0.3}$ interface to the total layer of $Ni_2Si_{0.7}Ge_{0.3}$, and finally accumulated at the surface of $NiSi_{0.7}Ge_{0.3}$. We found that under the assistance of Al atoms, the best quality Ni germanosilicide layer was achieved by annealing at 700 °C in the case of 3 nm Al.

Keywords: germanosilicide, Al, Ni

PACS: 85.30.Kk, 85.30.De, 85.30.Hi **DOI:** 10.1088/1674-1056/26/9/098503

1. Introduction

The nickel mono-silicide (NiSi) has been widely used in metal–oxide–semiconductor field effect transistor (MOSFET) due to its low resistivity, low Si consumption, and low formation temperature.[1–4] However, when Ni reacts with silicon–germanium alloy ($Si_{1-x}Ge_x$), it is difficult to form a uniform Ni–germanosilicide (NSG) layer due to the different heat formation between Ni–Si and Ni–Ge.[5,6] Furthermore, the poor thermal stability of the NSG layer and Ge-out diffusion from the NSG layer will induce the agglomeration of NSG grains, which brings large contact variations and leakage to the related $Si_{1-x}Ge_x$ devices.[7] $Si_{1-x}Ge_x$ is already employed in source/drain (S/D)[8] or channel areas of pMOSFETs,[9] so smooth and uniform $NSG/Si_{1-x}Ge_x$ interfaces are needed for device applications. In recent years, the solid-phase reactions of Ni with $Si_{1-x}Ge_x$ have been studied in detail.[10–12] The $NSG/Si_{1-x}Ge_x$ contact properties could be improved by several methods, such as ions pre-implanted into $Si_{1-x}Ge_x$,[13] introducing some other metal elements,[14–16] and different annealing processes.[17,18] Especially, Al incorporation is considered as a promising way to mediate the complex reactions between Ni and $Si_{1-x}Ge_x$.[19–22] Our previous results showed that an Al interlayer or $Ni_{1-x}Al_x$ alloy could greatly reduce the $NSG/Si_{1-x}Ge_x$ interface roughnesses.[19,21] Moreover, it has been reported that Al atoms could tune the hole Schottky barrier height at the $NSG/Si_{1-x}Ge_x$ junction to sub-0.1 eV.[23] Thus, the Al impact on germanosilicidation is interesting and needs further study. Liu *et al.* investigated the formation of Ni germanosilicide layers on strained $Si_{1-x}Ge_x$ with different Al contents in $Ni_{1-x}Al_x$ alloy.[24] However, in the case of Al interlayer, the effects of the Al thickness and annealing temperature on the formation of NSG are not fully understood. In this paper, we systematically investigate the solid reactions between Ni and relaxed $Si_{0.7}Ge_{0.3}$ substrate with different Al interlayer thicknesses under various annealing temperatures.

2. Experiment

The fully relaxed $Si_{0.7}Ge_{0.3}$ with a thickness of about 800 nm was deposited by reduced pressure chemical vapor deposition (RPCVD) on a Si (100) substrate with graded $Si_{1-y}Ge_y$ ($y < 0.3$) buffer layers. After standard RCA cleaning, $Si_{0.7}Ge_{0.3}$ samples were dipped in dilute HF solution (1%) to remove the native oxide. 1 nm and 3 nm Al interlayers were deposited on the $Si_{0.7}Ge_{0.3}$ substrate followed by subse-

*Project supported by the Natural Science Foundation of Shanghai, China (Grant No. 14ZR1418300) and the National Natural Science Foundation of China (Grant Nos. 61604094 and 61306126).

†Corresponding author. E-mail: xyping@sues.edu.cn

‡Corresponding author. E-mail: bozhang@mail.sim.ac.cn

© 2017 Chinese Physical Society and IOP Publishing Ltd

quent Ni layer with 10 nm thickness at room temperature, as schematically shown in Figs. 1(a) and 1(c). The metal thicknesses were confirmed by Rutherford backscattering spectrometry (RBS) using RUMP simulation[25] (see Figs. 1(b) and 1(d)). The $Si_{1-x}Ge_x$ films were so thick that the individual spectra of Ni, Al, Si, and Ge could not be resolved. Meanwhile, 10 nm Ni layer without Al was also deposited directly on the $Si_{0.7}Ge_{0.3}$ substrate for comparison. Ni germanosilicidation was formed by rapid thermal annealing (RTA) in ambient N_2 for 30 s at various temperatures ranging from 400 °C to 700 °C. The un-reacted Ni was selectively etched in solution H_2SO_4:H_2O_2 (1:4).

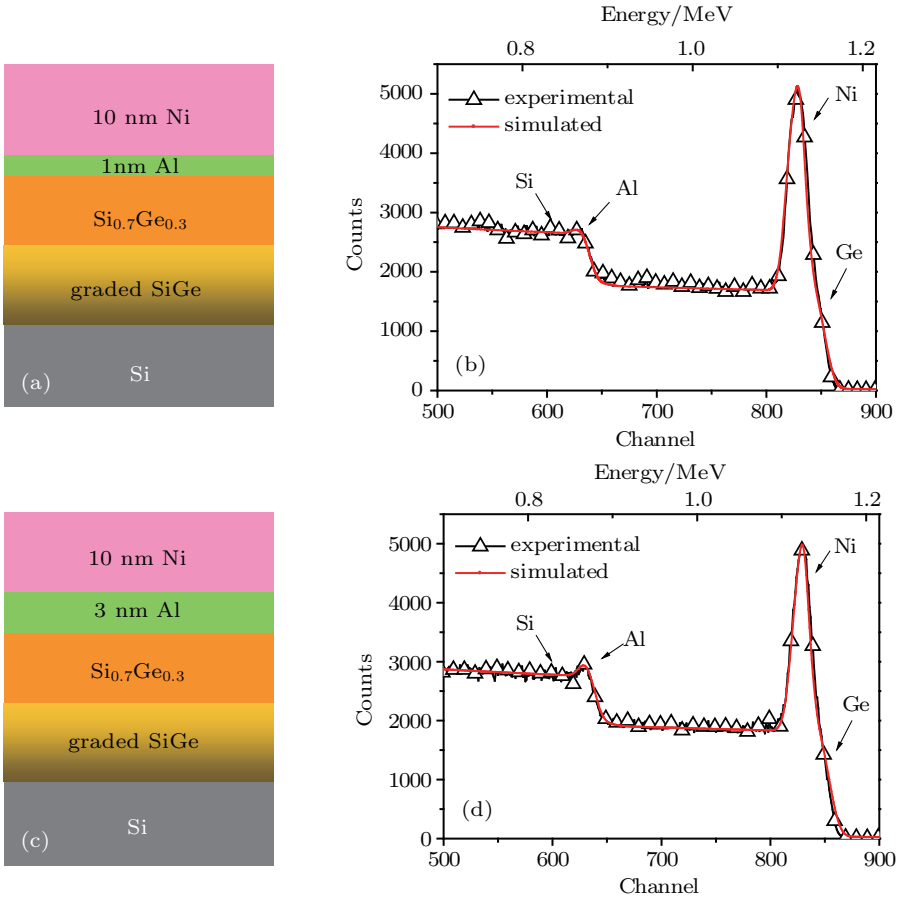


Fig. 1. (color online) Schematic diagrams of Ni/Al/SiGe systems and the corresponding RBS measurements: (a), (b) 1 nm Al; (c), (d) 3 nm Al.

The stoichiometry of the NSG layers was investigated by RBS. The simulations of the RBS spectra were made by means of RUMP. The morphology and microstructure were studied by cross-section transmission electron microscopy (XTEM) and scanning transmission electron microscopy (STEM). The elements redistributions were analyzed by secondary ion mass spectroscopy (SIMS).

3. Results and discussion

3.1. The stoichiometry of the NSG layers

The stoichiometry of the NSG layers was investigated by RBS with 1.4 MeV He^+ at a scattering angle of 170 °C. Figure 2 presents the RBS spectra of the NSG layers with or without (w/o) Al interlayer at different silicidation temperatures. For the samples w/o Al, based on the RUMP program (not shown), it is simulated that the proportion of Ni and $Si_{0.7}Ge_{0.3}$ is approximately 1:1 at 400 °C, indicating that the layer is in mono-germanosilicide phase ($NiSi_{0.7}Ge_{0.3}$). After high temperature annealing (600 °C), the composition of the NSG layer shows a great change indicated by the widening of the Ni signal and the raising of the Ge signal in the RBS spectrum, which means a rough NSG/$Si_{0.7}Ge_{0.3}$ interface and an inhomogeneous layer due to agglomeration. For the sample with 1 nm Al, at 400 °C, no significant difference to the sample w/o Al is found. At 600 °C, we can see some thermal stability improvements of the NSG layer due to the appearance of Al. However, according to the RUMP simulation (not shown), the Ge concentration in the NSG layer is higher than that in the mono $NiSi_{0.7}Ge_{0.3}$ phase, indicating that the Ge atoms are already diffused from $NiSi_{0.7}Ge_{0.3}$ polycrystalline grains. In the case of 3 nm Al, the RBS random spectrum of the sample annealed at 500 °C can be simulated by an 18.5 nm thick $Ni_2Si_{0.7}Ge_{0.3}$ layer. After annealing at 600 °C, a mixture of phases ($Ni_2Si_{0.7}Ge_{0.3}$ and $NiSi_{0.7}Ge_{0.3}$) is found according to the RUMP simulation. These phases can totally transfer to the

mono-$NiSi_{0.7}Ge_{0.3}$ phase when the annealing temperature is increased to 700 °C. Most of the Al is found in a ~4 nm thick oxidized Al top layer (see Fig. 2(c)). Based on these results, we conclude that the appearance of Al retards the Ni-rich germanosilicide phase to the mono-germanosilicide phase.

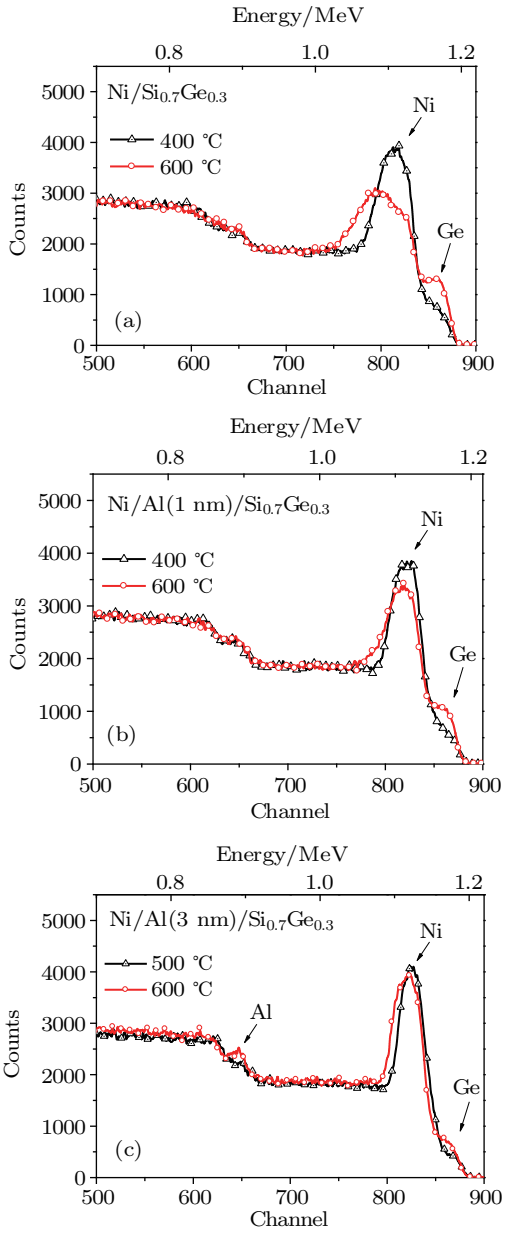


Fig. 2. (color online) RBS spectra of NSG layers formed at different temperatures: (a) w/o Al, (b) 1 nm Al, (c) 3 nm Al.

3.2. Morphology dependence on Al thickness

In order to study the difference in morphology between $Ni/Si_{0.7}Ge_{0.3}$ and $Ni/Al/Si_{0.7}Ge_{0.3}$ systems, XTEM was employed to analyze the samples with and w/o Al (as shown in Fig. 3). For the sample w/o Al and after annealing at 400 °C, polycrystalline NSG grains are formed, which cause rough surface and interface of the layer (Fig. 3(a)). The incorporation of Al can reduce the roughness of both the surface and the interface of the $NiSi_{0.7}Ge_{0.3}$ layer. 1 nm Al interlayer is sufficient for the suppression of NSG grains formation at the surface, as revealed by the TEM micrograph in Fig. 3(b). The layer uniformity and interface roughness are improved compared to the case of Al absence. 3 nm Al interlayer results in the NSG layer with a very sharp interface (Fig. 3(c)). Note that there are still a few $Ni_2Si_{0.7}Ge_{0.3}$ grains inside the $NiSi_{0.7}Ge_{0.3}$ layer, which means that the Ni-rich germanosilicide phase is not totally transformed to the mono-germanosilicide phase even under high-temperature annealing. The existence of $Ni_2Si_{0.7}Ge_{0.3}$ grains increases the surface roughness of the $NiSi_{0.7}Ge_{0.3}$ layer. These results are consistent with the RBS measurements shown in Fig. 2(c), which further proves the appearance of Al can retard the mono-germanosilicide phase formation.

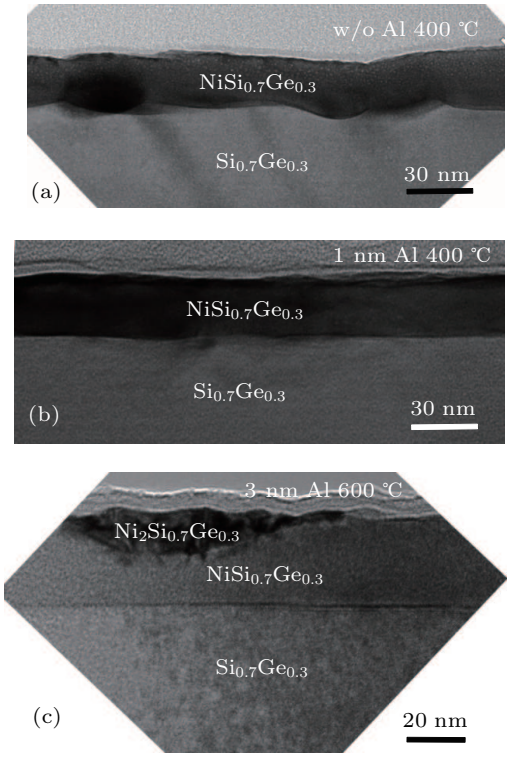


Fig. 3. XTEM images of NSG layers: (a) w/o Al at 400 °C, (b) 1 nm Al at 400 °C, (c) 3 nm Al at 600 °C.

3.3. Dependence on annealing temperature

In this section, we discuss the annealing temperature dependence of the NSG formation with 3 nm Al interlayer. The STEM micrographs in Fig. 4 depict the morphology of the NSG layers formed at various annealing temperatures. The NSG layer formed at 500 °C has the average thickness of ~ 19 nm with $Ni_2Si_{0.7}Ge_{0.3}$ phase corresponding to the RBS simulation (Fig. 2(c)). After annealing at 550 °C, the number of polycrystalline NSG grains is reduced and the NSG layer uniformity and the interface morphology are improved. With the annealing temperature increasing to 700 °C, the NSG layer has totally transferred to the mono $NiSi_{0.7}Ge_{0.3}$ phase with the thickness of ~ 24 nm, as demonstrated by the bright

uniform layer in Fig. 4(c). Due to the lack of $Ni_2Si_{0.7}Ge_{0.3}$ polycrystalline grains, the surface of the $NiSi_{0.7}Ge_{0.3}$ layer becomes very smooth with a sharp $NiSi_{0.7}Ge_{0.3}/Si_{0.7}Ge_{0.3}$ interface. In order to further investigate the temperature dependence, high-resolution XTEM (HRTEM) was performed for samples annealed at 500 °C, 550 °C, 600 °C, and 700 °C respectively. Figure 5(a) displays the sample annealed at 500 °C with several different orientation $Ni_2Si_{0.7}Ge_{0.3}$ polycrystalline grains, which cause the surface and interface of the $Ni_2Si_{0.7}Ge_{0.3}$ layer to be very rough. After 550 °C annealing, the $Ni_2Si_{0.7}Ge_{0.3}$ layer starts to become uniform with smooth interface, although the atomic steps still exist (see Fig. 5(b)). At 600 °C, main $Ni_2Si_{0.7}Ge_{0.3}$ has transformed to $NiSi_{0.7}Ge_{0.3}$ and only a few $Ni_2Si_{0.7}Ge_{0.3}$ grains still exist in the $NiSi_{0.7}Ge_{0.3}$ layer, as shown in Fig. 3(c). After 700 °C annealing, the $NiSi_{0.7}Ge_{0.3}$ layer has a uniform thickness over the entire viewable area. The interface between $NiSi_{0.7}Ge_{0.3}$ and $Si_{0.7}Ge_{0.3}$ substrate is sharp and flat without evidence of the formation of any second phase. As reported earlier in Ref. [19], this $NiSi_{0.7}Ge_{0.3}$ layer is epitaxial growth on the (001) $Si_{0.7}Ge_{0.3}$ substrate with the (101) orientation.

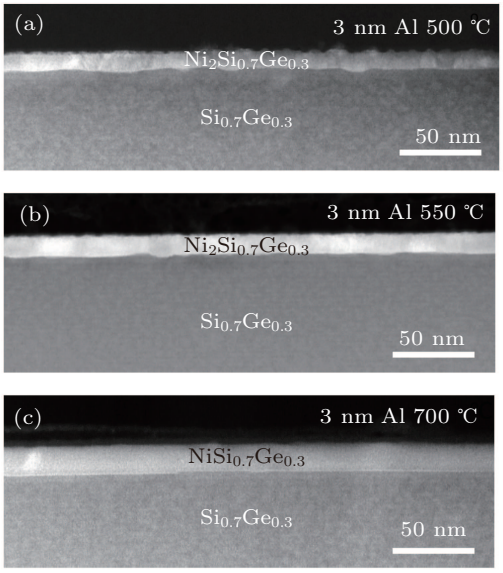


Fig. 4. STEM images of NSG layers formed with 3 nm Al at different annealing temperatures: (a) 500 °C, (b) 550 °C, (c) 700 °C.

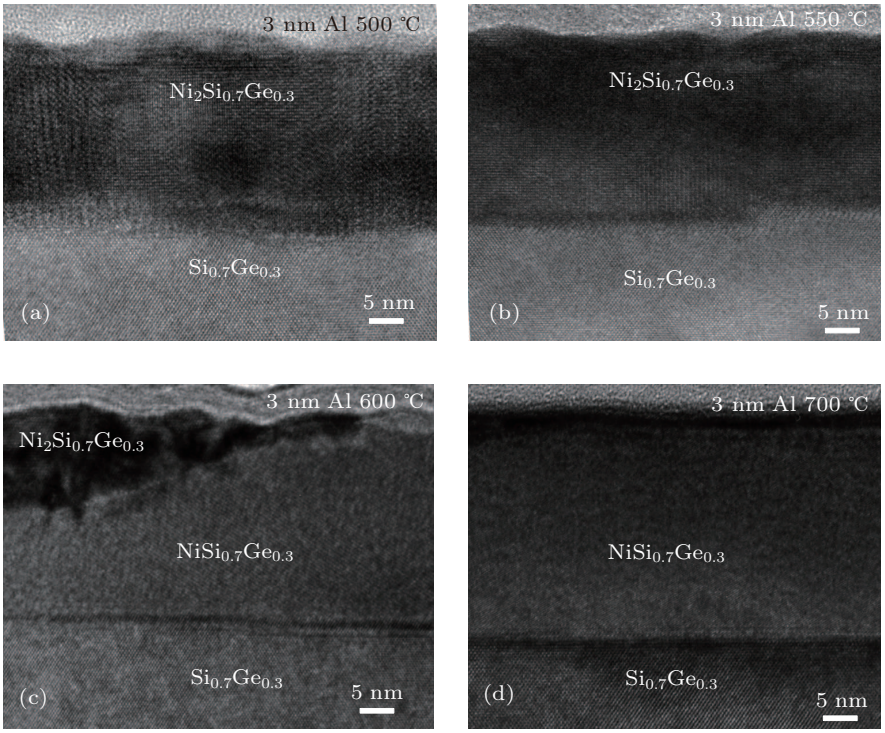


Fig. 5. High resolution XTEM images of NSG layers formed with 3 nm Al at different annealing temperatures: (a) 500 °C, (b) 550 °C, (c) 600 °C, (d) 700 °C.

3.4. Al redistribution after germanosilicidation

To clarify the exact role of Al atoms on the germanosilicidation process, we utilized SIMS to monitor the Al, Ni, Si, Ge depth profiles in the 3 nm Al samples annealed at different temperatures. Note that the results in Fig. 6(d) are a reproduction from Ref. [22] in order to facilitate a direct comparison. As shown in Fig. 6(a), at the annealing temperature of 500 °C, the flat Ni plateaus indicate the formation of single $Ni_2Si_{0.7}Ge_{0.3}$ phase. The Al distribution is also very uniform in the NSG layer, indicating that main Al atoms are expelled from the interlayer to the NSG layer during the Ni-$Si_{0.7}Ge_{0.3}$ reaction. After 550 °C annealing, some Al atoms start to move to the surface and finally form an obvious pileup of Al on the upper of the NSG layer. Consequently, the NSG layer maybe

splits into two sub-layers: one layer located closer to the unreacted $Si_{0.7}Ge_{0.3}$ substrate, and the other layer adjacent to the surface with a much higher Al concentration. Moreover, we find that there are some Si and Ge atoms accumulations at the interface of NSG/$Si_{0.7}Ge_{0.3}$ in both 500 °C and 550 °C annealing samples. However, with further increasing annealing temperature to 600–700 °C, Si and Ge atoms accumulations disappear and most Al atoms segregate at the surface of the NSG layer. Furthermore, we note that the redistributions of the Ni/Al/Si/Ge signals in the NSG layers do not change after annealing at 600–700 °C due to the formation of the most stable mono-gemanosilicide phase. The minor difference of the SIMS depth files at 600 °C and 700 °C is the remaining Al atoms distributions in the oxide layer on the top of the NSG layers. Although a few Ni-rich germanosilicide grains are formed in the NSG layer at 600 °C (as shown in Fig. 5(c), it is found that they have marginal impacts on the Ni/Al/Si/Ge contents in the NSG layer.

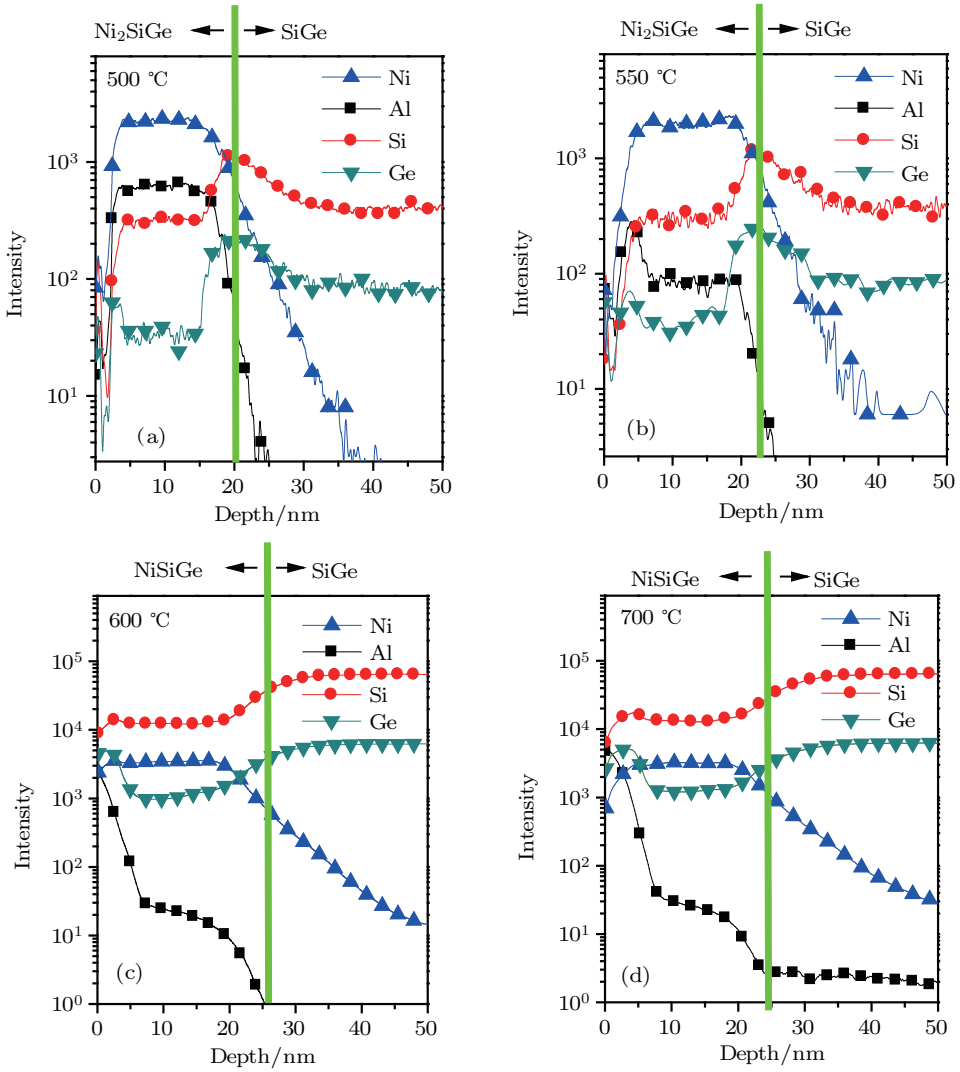


Fig. 6. (color online) SIMS results of NSG layers formed with 3 nm Al at different annealing temperatures: (a) 500 °C, (b) 550 °C, (c) 600 °C, (d) 700 °C.

3.5. Sheet resistance measurements

The impact of the Al interlayer on the NSG electrical properties was investigated by sheet resistance measurements. The annealing temperature dependence of the sheet resistance for the samples with or w/o Al is shown in Fig. 7. Note that the data have been partially shown in Ref. [19] and they are reproduced here only for comparison with the case of 1 nm Al interlayer. For Ni/$Si_{0.7}Ge_{0.3}$ and Ni/Al(1 nm)/$Si_{0.7}Ge_{0.3}$ systems, the R_s keeps at the value of ~ 7 Ω/sq from 400 °C to 500 °C, indicating the formation of mono-germanosilicide phase. The layer suffers pronounced degradation when the temperature increases above 500 °C. However, for the Ni/Al(3 nm)/$Si_{0.7}Ge_{0.3}$ system, the sheet resistance remains at a higher value at 400–500 °C due to the formation of a Ni-rich germanosilicide phase, as shown in Figs. 5 and 6. The sheet resistance then decreases abruptly after annealing at 500 °C, which is attributed to the transformation of Ni-rich germanosilicide phase to mono-germanosilicide phase. The thermal stability of the NSG layer increases up to 700 °C. It is evident that the incorporation of 3 nm Al retards the phase for-

mation and enhances the thermal stability of the germanosilicide layer.

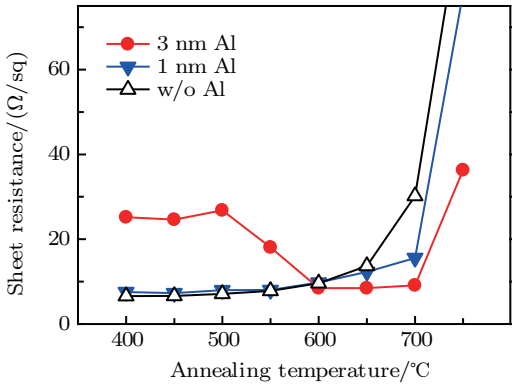


Fig. 7. (color online) Sheet resistance of NSG layers formed with and w/o Al interlayer versus annealing temperature.

3.6. Discussion

Based on the structural and electrical analysis, we now discuss the effects of the Al interlayer on the growth mechanism of $NiSi_{0.7}Ge_{0.3}$ on $Si_{0.7}Ge_{0.3}$. In the case of Si substrate, the addition of Al decreases the disilicide formation temperature and leads to a uniform orientation of the disilicide layers, which depend on the Al content and annealing temperature.[26] However, for the $Si_{0.7}Ge_{0.3}$ substrate, the incorporation of Al increases the mono-germanosilicide formation temperature and finally mediates the NSG layer with smooth interface. The Al interlayer behaves as a diffusion barrier to reduce the diffusion of Ni and induces the formation of a uniform NSG layer. Considering the difference of 1 nm and 3 nm Al on the formation of $NiSi_{0.7}Ge_{0.3}$, as shown in Figs. 3(b) and 3(c), we find that the appearance of enough Al atoms could reduce and balance the reaction of Ni and $Si_{0.7}Ge_{0.3}$, inducing a uniform epitaxial growth of $NiSi_{0.7}Ge_{0.3}$ on $Si_{0.7}Ge_{0.3}$. In addition, Jin *et al.* found that the surface and interface energies of NiSiGe could be minimized for highly (200) orientation by the addition of 5% Pd in NiPd alloy.[16] We propose that Al atoms have the same effect, i.e., lowering the dominant interface and surface energies, indicating that $NiSi_{0.7}Ge_{0.3}$ with favorable orientation may grow faster than $NiSi_{0.7}Ge_{0.3}$ with other orientations.

4. Conclusion

The formation of NSG layers is systematically investigated with different annealing temperatures in the appearance of Al. It is shown that both the Al interlayer thickness and annealing temperature could greatly affect the Ni-$Si_{0.7}Ge_{0.3}$ reaction. The incorporation of Al improves the surface and interface morphology of the NSG layers, enhances the thermal stabilities, and retards the mono-germanosilicide phase formation. In the case of 3 nm Al, a very uniform and smooth $NiSi_{0.7}Ge_{0.3}$ layer is formed after 700 °C annealing. The Al atoms distribute from the Ni/$Si_{0.7}Ge_{0.3}$ interface to the total layer of $Ni_2Si_{0.7}Ge_{0.3}$, and finally accumulate at the surface of the $NiSi_{0.7}Ge_{0.3}$ layer. These results indicate that the combined process of Al interlayer may serve as a potential method for improving the contact properties of $NiSi_{1-x}Ge_x/Si_{1-x}Ge_x$.

References

[1] Zhang S L and Östling M 2013 *Criti. Rev. Solid State* **28** 1

[2] Lavoie C, d'Heurle F M, Detavernier C and Cabral J C 2003 *Microelectron. Eng.* **70** 144

[3] Luo J, Qiu Z, Zha C, Zhang Z, Wu D, Lu J, Åkerman J, Östling M, Hultman L and Zhang S L 2010 *Appl. Phys. Lett.* **96** 031911

[4] Luo J, Qiu Z, Zha C, Zhang Z, Östling M and Zhang S L 2010 *J. Vac. Sci. Technol. A* **28** C1I1

[5] Zhang S L 2003 *Microelectron. Eng.* **70** 174

[6] Li J, Hong Q Z, Mayer J W and Rathbun L 1990 *J. Appl. Phys.* **67** 2506

[7] Liu J and Ozturk M C 2005 *IEEE Trans. Electron Devices* **52** 1535

[8] Packan P, Akbar S, Armstrong M, Bergstrom D, Brazier M, Deshpande H, Dev K, Ding G, Ghani T, Golonzka O, Han W, He J, Heussner R, James R, Jopling J, Kenyon C, Lee S H, Liu M, Lodha S, Mattis B, Murthy A, Neiberg L, Neirynck J, Pae S, Parker C, Pipes L, Sebastian J, Seiple J, Sell B, Sharma A, Sivakumar S, Song B, Amour A St, Tone K, Troeger T, Weber C, Zhang K, Luo Y and Natarajan S 2009 *IEDM Tech. Dig.* 659

[9] Yu W, Zhang B, Zhao Q T, Hartmann J M, Buca D, Nichau A, Lupták R, Lopes J M, Lenk S, Luysberg M, Bourdelle K K, Wang X and Mantl S 2011 *Solid State Electron.* **62** 85

[10] Jin L, Pey K L, Choi W K, Fitzgerald E A, Antoniadis D A, Pitera A J, Lee M L, Chi D Z, Rahman M A, Osipowicz T and Tung C H 2005 *J. Appl. Phys.* **98** 033520

[11] Jarmar T, Seger J, Ericson F, Mangelinck D, Smith U and Zhang S L 2002 *J. Appl. Phys.* **92** 7193

[12] Pey K L, Choi W K, Chattopadhyay S, Zhao H B, Fitzgerald E A, Antoniadis D A and Lee P S 2002 *J. Vac. Sci. Technol. A* **20** 1903

[13] Zhang B, Yu W, Zhao Q T, Buca D, Holländer B, Hartmann J M, Zhang M, Wang X and Mantl S 2011 *Electrochem. Solid-State Lett.* **14** H261

[14] Xu Y, Ru G, Jiang Y, Qu X and Li B 2009 *Appl. Surf. Sci.* **256** 305

[15] Liu Q, Wang G, Guo Y, Ke X, Liu H, Zhao. C and Luo J 2015 *Vacuum* **111** 114

[16] Jin L, Pey K L, Choi W K, Fitzgerald E A, Antoniadis D A, Pitera A J, Lee M L and Tung C H 2005 *J. Appl. Phys.* **97** 104917

[17] Setiawan Y, Lee P S, Pey K L, Wang X C, Lim G C and Tan B L 2007 *Appl. Phys. Lett.* **90** 073108

[18] Hu C, Xu P, Fu C, Zhu Z, Gao X, Jamshidi A, Noroozi M, Radamson H, Wu D and Zhang S L 2012 *Appl. Phys. Lett.* **101** 092101

[19] Zhang B, Yu W, Zhao Q T, Mussler G, Jin L, Buca D, Hollaender B, Zhang M, Wang X and Mantl S 2011 *Appl. Phys. Lett.* **98** 252101

[20] Zhao Q T, Knoll L, Zhang B, Buca D, Hartmann J and Mantl S 2013 *Microelectron. Engineering.* **107** 190

[21] Liu L, Jin L, Knoll L, Wirths S, Nichau A, Buca D, Mussler G, Holländer B, Xu D, Di Z, Zhang M, Zhao Q and Mantl S 2013 *Appl. Phys. Lett.* **103** 231909

[22] Ping Y X, Wang M L, Meng X R, Hou C L, Yu W L, Xue Z Y, Wei X, Zhang M, Di Z F and Zhang B 2016 *Acta Phys. Sin.* **65** 036801 (in Chinese)

[23] Sinha M, Lee R T P, Lohani A, Mhaisalkar S, Chor E F and Yeo Y C 2009 *J. Electrochem. Soc.* **156** 233

[24] Liu L J, Jin L, Knoll L, Wirths S, Buca D, Mussler G, Hollaender B, Xu D W, Di Z F, Zhang M, Mantl S and Zhao Q T 2015 *Microelectron. Eng.* **137** 88

[25] Doolittle L 1985 *Nucl. Inst. Meth. B* **9** 344

[26] Mogilatenko A, Beddies G, Falke M, Hausler I and Neumann W 2012 *J. Appl. Phys.* **111** 103512